Cell, Vol. 92, 193–204, January 23, 1998, Copyright ©1998 by Cell Press

An Anaphase Calcium Signal Controls Chromosome Disjunction in Early Sea Urchin Embryos

Laurence Groigno† and Michael Whitaker*
Department of Physiological Sciences
University of Newcastle Upon Tyne
Medical School
Newcastle Upon Tyne NE2 4HH
United Kingdom

Summary

A transient increase in intracellular calcium concentration $[Ca^{2+}]_i$ occurs throughout the cell as sea urchin embryos enter anaphase of the first cell cycle. The transient just precedes chromatid disjunction and spindle elongation. Microinjection of calcium chelators or heparin, an $InsP_3$ receptor antagonist, blocks chromosome separation. Photorelease of calcium or $InsP_3$ can reverse the block. Nuclear reformation is merely delayed by calcium antagonists at concentrations that block chromatid separation. Thus, the calcium signal triggers the separation of chromatids, while calcium-independent pathways can bring about the alterations in microtubule dynamics and nuclear events associated with anaphase progression. That calcium triggers chromosome disjunction alone is unexpected. It helps explain previous conflicting results and allows the prediction that calcium plays a similar role at anaphase in other cell types.

Introduction

The cell division cycle employs finely balanced control mechanisms to ensure that genetic information is copied faithfully and transmitted from mother to daughter cells. Perhaps the most striking example of this is at mitosis, where the sister chromatids assemble at the metaphase plate of the mitotic spindle before separating and moving to the spindle poles at anaphase. In insect spermatocytes, anaphase onset can be delayed by detaching a single chromosome (Nicklas et al., 1995), suggesting that a spindle assembly cell cycle checkpoint exists just before anaphase onset.

Checkpoints are also found before other key events in the cell cycle (reviewed in Hartwell and Weinert, 1989; Murray, 1992; Elledge, 1996). The idea is that certain preconditions must be met before the cell can safely proceed to the next stage of the cell cycle. The molecular basis of these checks to cell cycle progression has begun to be understood (reviewed in King et al., 1994; Nurse, 1994; Elledge, 1996; Nasmyth, 1996). In the case of anaphase onset, it appears that release of the checkpoint mechanism leads to activation of the anaphase-promoting complex (APC or cyclosome), a ubiquitinating heteromer linked to proteasome-mediated proteolysis (reviewed in King et al., 1996). Activation of the APC causes proteolysis of mitotic cyclins and is also essential for disjunction of sister chromatids, but disjunction and cyclin destruction can be dissociated (Holloway et al., 1993; Surana et al., 1993; Yamano et al., 1996).

How a cell senses that the chromatids are well assembled on a mitotic spindle is, to some extent, understood (Rieder et al., 1994; Li and Nicklas, 1995), but the molecular link between the spindle checkpoint and activation of the APC/proteasome pathway has not been discovered. In general terms, it is thought that the ubiquitin-dependent proteolytic system may be activated by the mitotic kinase itself, so that kinase activation leads inevitably to cyclin destruction and loss of kinase activity (Félix et al., 1990; Luca et al., 1991; Herschko et al., 1994). However, there are other models available that might explain activation of the APC. These involve the calcium-signaling system.

The clearest example of calcium's involvement in anaphase onset comes from fertilization in *Xenopus* oocytes. Fertilization is accompanied by a large calcium transient that leads first to cyclin destruction (Lorca et al., 1991, 1993), presumably through activation of the APC/proteasome pathway (Whitaker, 1993). These experiments indicate that, at least in the special case of fertilization, a calcium signal can lead to stimulation of APC activity and exit from meiosis.

There is longstanding evidence that calcium may also regulate anaphase onset at mitosis in somatic cells. In 1983, Izant showed that anaphase in PtK1 cells could be advanced by microinjecting calcium and delayed by injecting calcium–EGTA buffers. Izant concluded that an increase in $[Ca^{2+}]_i$ during metaphase might stimulate anaphase onset but did not act directly on kinetochores. The development of the fluorescent calcium indicator fura2 (Poenie et al., 1985) allowed the detection of brief calcium increases at anaphase onset in mammalians cells (Poenie et al., 1986; Rattan et al., 1986). However, these calcium transients were shown to occur several minutes before anaphase onset was detected (Rattan et al., 1988). They could be suppressed by removing serum or calcium from the extracellular medium without affecting the progression of mitosis in Swiss 3T3 cells (Tombes and Borisy, 1989). Tombes and Borisy (1988) also showed that a serum-independent steady rise in $[Ca^{2+}]_i$ accompanied anaphase onset. Indeed, EGTA and BAPTA blocked anaphase onset only in calcium-free medium, a condition in which the sustained $[Ca^{2+}]_i$ increase was suppressed. The dissociation of calcium spikes and anaphase onset was confirmed in REF52 cells and Swiss 3T3 fibroblasts (Kao et al., 1990). Serum removal and permeant BAPTA abolished the calcium spikes without preventing anaphase onset. Photolysis of a caged calcium chelator to generate a calcium pulse, an approach used successfully to induce premature nuclear envelope breakdown (NEB), did not alter the timing of the metaphase-anaphase transition when delivered at metaphase in these fibroblasts (Kao et al., 1990). Present evidence in mammalian cell lines thus leaves

*To whom correspondence should be addressed.
†Present address: UPRES-A 6026 CNRS, Biologie Cellulaire et Reproduction, Université de Rennes, 1. Campus de Beaulieu, Av. du General Leclerc, 35042 Rennes Cedex, France.

the question of calcium's involvement at anaphase unresolved, though it is evident that a calcium signal is essential for entry into mitosis (Lu and Means, 1993; Hepler, 1994).

In the plant *Tradescantia*, exit from metaphase was also delayed in stamen hair cells by removing extracellular calcium (Hepler, 1985). However, a slow increase in $[Ca^{2+}]_i$ was detected only after anaphase onset (Hepler and Callaham, 1987). The calcium rise was proposed to contribute to anaphase chromosome movement since movement was slowed by chelating external calcium (Zhang et al., 1992).

The sea urchin embryo has been a very useful model in providing solid evidence that a premitotic calcium signal triggers entry into mitosis (Poenie et al., 1985; Steinhardt and Alderton, 1988; Twigg et al., 1988; Wilding et al., 1996) and is a useful cell type for testing whether calcium participates in the control of anaphase onset. Levels of the calcium-releasing messenger $InsP_3$ increase at anaphase (Ciapa et al., 1994) and peaks of $[Ca^{2+}]_i$ occur just before mitosis and around anaphase (Poenie et al., 1985; Ciapa et al., 1994; Wilding et al., 1996). The phosphoinositide antagonist lithium blocks anaphase (Becchetti and Whitaker, 1997), as does the calcium-binding dye antipyralazoIII (Silver, 1989). Using confocal imaging to follow spatio-temporal calcium variations and spindle morphology, we report here that a calcium transient occurs just before anaphase during the first cell cycle of the sea urchin embryo. Chelating calcium reversibly blocks chromosome separation. The $[Ca^{2+}]_i$ transient is $InsP_3$ mediated, in that it is absent in embryos microinjected with heparin, an $InsP_3$ receptor antagonist. Heparin reversibly and completely blocks chromatid disjunction. We therefore demonstrate that an anaphase calcium signal controls chromatid separation.

Results

Ratiometric Confocal Calcium Imaging Detects a Global Anaphase-Related Calcium Signal

Using dextran dye–based ratiometric imaging methods, we find that calcium increases abruptly at around the time of anaphase onset (Figures 1A and 1B). The anaphase-related calcium transient is larger (323 $\pm$ 27 nM, mean and SEM, n = 15) than the transient that triggers NEB (Wilding et al., 1996). $[Ca^{2+}]_i$ increases throughout the embryo (Figure 1A), rising to a peak in 1–2 min. In 7 of the 15 embryos, $[Ca^{2+}]_i$ fell back toward resting levels over 2–7 min before rising again as cytokinesis occurred (Figures 1A and 1B). In 8 of the 15, the anaphase-associated transient was longer, falling slowly back to resting levels after cytokinesis. In three further experiments at an enhanced sampling frequency (14 s rather than 28 s), the anaphase-associated transient could be resolved into a series of peaks resembling a damped oscillation (Figure 1E).

Although $[Ca^{2+}]_i$ increased throughout the embryo in all experiments, in 15 of the 18 cases $[Ca^{2+}]_i$ was detectably lower in the vicinity of the spindle than in the cortex (Figure 1C). Yet when the spatial $[Ca^{2+}]_i$ distribution at the peak of the transient is compared with the $[Ca^{2+}]_i$ distribution at the base of the transient by normalizing the peak distribution to the spatial distribution at the base, the increase is uniform (Figure 1D). This transform indicates that the proportionate increase in $[Ca^{2+}]_i$ is spatially uniform and suggests that a standing gradient of calcium is maintained in the embryo throughout anaphase with lower $[Ca^{2+}]_i$ in the region of the mitotic spindle. The standing gradient (and, indeed, the anaphase-associated transient) was also seen in embryos dividing in calcium-free sea water (not shown). No gradients in the signal could be detected when a fluorescein dextran/rhodamine dextran couple was substituted for the calcium green dextran/rhodamine dextran ratio pair—an internal control for the ratio method itself (not shown).

Determining the Time of Anaphase Onset

Because the precise timing of anaphase onset is hard to judge using conventional microscopy, we used the Hoechst 33342 DNA dye and microinjected rhodamine tubulin during G2 of the first cell cycle to determine suitable parameters of anaphase onset in sea urchin embryos. Spindle morphology and chromatid separation were recorded simultaneously by dual laser line confocal microscopy (Figure 2). When stained with the Hoechst dye and illuminated with UV light, one or two chromosomes showed a slight delay in separation (Figure 2A). However, chromosome movements toward the spindle poles were readily visible and complete separation of both chromosome sets was always observed. Growth of the spindle asters could also be observed; the asters appear to enlarge due to microtubule elongation and from a reorganization and enlargement of the pericentriolar material (Figure 2A). To determine the relative timing of these events, the area of the image occupied by the chromosomes was measured (CA), along with the spindle pole–pole distance (P–P) and the astral microtubule bundle length (AMT). These parameters should report chromatid separation, spindle elongation, and growth of the asters. The time course of the changes in these parameters during mitosis is shown in Figure 2B. All three parameters increase abruptly in mid-mitosis. We took the onset of the increases to be the time at which a significant increase was followed by three additional values that also differed significantly from the baseline (Figure 2B, arrows). The time resolution of these experiments was 36 s. In three of five embryos, the onset of chromatid separation (increase of CA) and pole–pole elongation occurred in the same frame, while in the remaining two embryos, the increase in pole–pole separation occurred one frame earlier (Figure 1C). The onset of astral microtubule bundle growth was not well correlated with the onset of an increase in either of the other two parameters and could occur many frames before or after (Figure 1D).

We concluded that the onset of pole–pole separation was a good proxy for chromosome disjunction, observed as chromosome separation.

The Anaphase-Related Calcium Transient Precedes the Onset of Spindle Elongation

Simultaneous records of $[Ca^{2+}]_i$ and spindle pole–pole distance were made in a further 14 embryos, using a

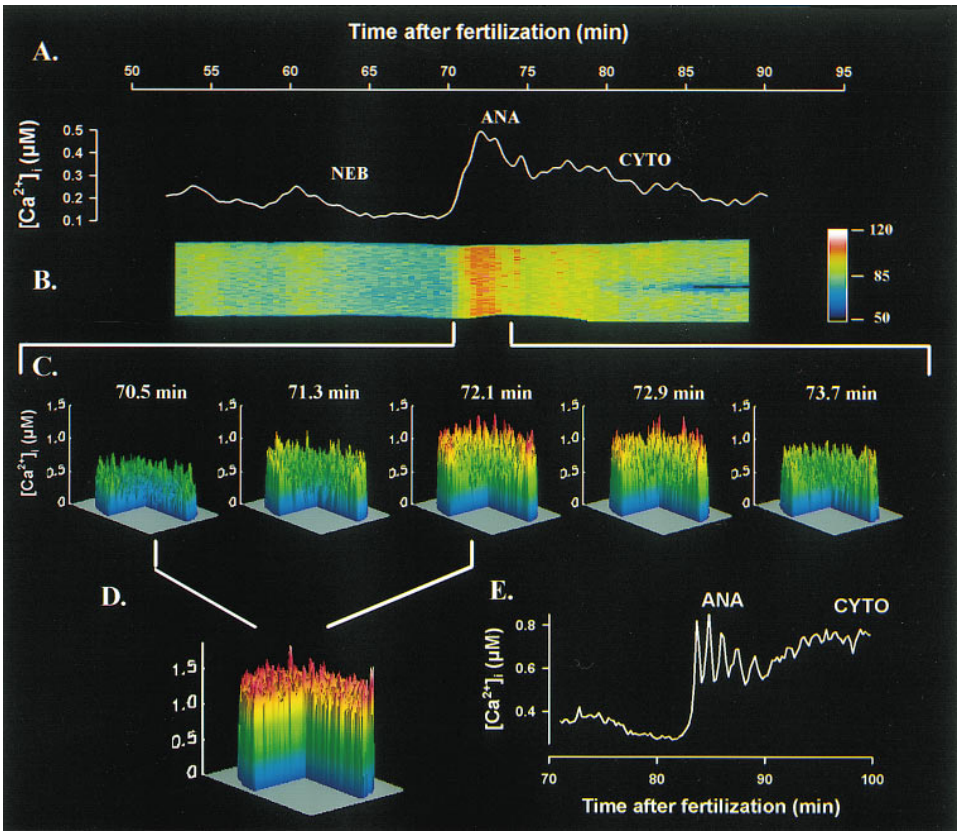

Figure 1. Global $[Ca^{2+}]_i$ Increase Associated with the Metaphase-Anaphase Transition

(A–D) $[Ca^{2+}]_i$ variations measured by confocal ratio-imaging. The embryo was injected in G2 with a CaGr/TMR mix. The figure displays the result obtained in one embryo. $[Ca^{2+}]_i$ fell back toward resting levels before increasing again at cytokinesis (representative of 7 out of 15 embryos, see text). Signals from both fluorescent dyes were recorded simultaneously every 24 s from late G2 until the end of cytokinesis (CYTO). (A) Calibrated $[Ca^{2+}]_i$ trace obtained from the ratio images and (B) waterfall plot, in which the $[Ca^{2+}]_i$ signal projected onto a single scan line through the center of the cell is monitored over time. Both show an increase in $[Ca^{2+}]_i$ at the beginning of anaphase (ANA). (C) Topograpical plot (ratio in a single confocal xy section plotted on z axis) of alternate data captures from 71 to 75 min showing that the calcium gradient from the spindle toward the cell periphery is maintained during anaphase. (D) Ratio between the first and the third image in (C) indicating that the relative $[Ca^{2+}]_i$ increase is uniform.

(E) Calcium oscillations detected at anaphase onset using higher sampling frequency (14 s between each image).

calcium green dextran pseudoratio (for explanation, see Experimental Procedures) and rhodamine-tubulin labeling of microtubules (Figure 3). Again, around half (8/15) manifested an isolated anaphase-associated $[Ca^{2+}]_i$ transient, while the others showed a similar rise to peak but a decline that was prolonged into cytokinesis (Figure 3B). We correlated the onset of the $[Ca^{2+}]_i$ transient with the onset of spindle elongation. In 11 cases, the onset of the $[Ca^{2+}]_i$ transient preceded spindle elongation or, in three cases, occurred in the same frame (Figure 3C). The timing of the $[Ca^{2+}]_i$ peak also correlated well with the onset of spindle elongation (Figure 3D).

In 2 of the 14 cases, a smaller calcium transient preceded the anaphase-associated transient by 5–7 min. These may represent abortive attempts at anaphase onset.

Calcium Chelators Prevent Chromosome Segregation

The close temporal correlation between the anaphase-related $[Ca^{2+}]_i$ signal and anaphase onset suggests that the $[Ca^{2+}]_i$ transient is the trigger for anaphase onset. To test this hypothesis, we microinjected embryos with dibromoBAPTA just after NEB, as the mitotic spindle was forming. DibromoBAPTA has been found to be the most effective calcium chelator for the purposes of suppressing calcium transients and gradients (Speksnijder et al., 1989; Lindsay et al., 1995). The effects of the chelator were graded and dose dependent (Table 1; Figure 4A). We observed four outcomes: divided cells with two nuclei (2 nu 2 cells), undivided cells with two nuclei (2 nu 1 cell), undivided cells with one nucleus (1 nu 1 cell), and undivided cells with condensed chromosomes (cc 1 cell). At all concentrations except the highest (600 μM), microtubules assembled normally to form a mitotic spindle. These results indicate that chromosome separation and cytokinesis are sensitive to calcium chelation. In cells in which only one nucleus formed, it was located either centrally or eccentrically. An eccentric location implies that unequal traction has been exerted on the chromatin by the spindle. At the highest dibromoBAPTA concentration, however, cells often took on a granular appearance (Figure 4A, 4); the absence of spindle and the block of chromatin decondensation may be

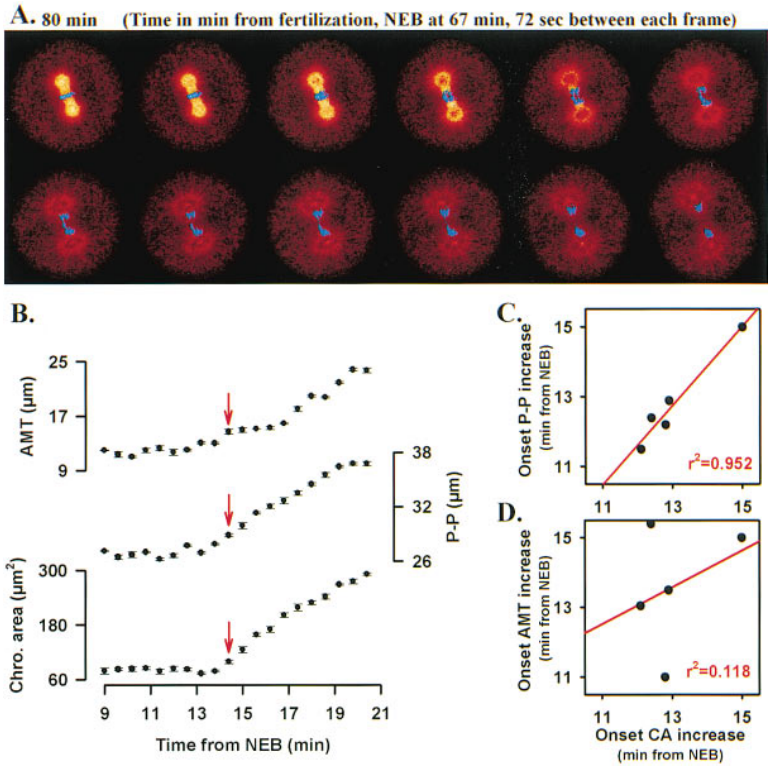

Figure 2. Real Time Imaging of the Spindle and the Chromosomes at Anaphase Onset in the Sea Urchin Embryo

(A) Time lapse confocal imaging of the metaphase-anaphase transition with simultaneous visualization of the microtubules (stained by injecting rhodamine-labeled tubulin) and DNA (Hoeschst 33342 staining). Sampling every 36 s (alternate combined images displayed).

(B) Variations of the distance between the two poles (P–P), the length of the astral microtubules (AMT), and the area occupied by the chromosomes (CA) at the metaphase-anaphase transition, measured from confocal images (n = 3, ± SEM, representative of five experiments). The times when each parameter begins to increase are indicated (red arrows), defined as the time after which at least three other points were significantly greater than the preceding point.

(C and D) Regression analysis comparing the onset of chromosome separation (onset CA) with the onset of pole–pole (P–P) increase (C) or with the onset of AMT increase (D). The regression coefficient, r^2, and the regression line are displayed in red on each graph.

due to rather more general inhibition of cell function and were not investigated further.

We saw similar effects with nitrophenyl-EGTA (NP-EGTA), another calcium chelator (Figures 4B and 4C). NP-EGTA blocked chromosome separation and cleavage without inhibiting formation of the spindle or preventing spindle elongation or reformation of the nucleus. NP-EGTA has the advantage that a proportion of the chelator can be photolysed by applying a pulse of UV light, releasing calcium into the cytoplasm (Wilding et al., 1996). Having suppressed the endogenous $[Ca^{2+}]_i$ transient, an exogenous calcium signal can be induced by photolysis of the chelator (Wilding et al., 1996). It is not possible to stain the chromosomes with Hoechst dye at these levels of UV light exposure, so the effects were followed with interference contrast optics. Eccentric nuclei were observed with NP-EGTA as they were with BAPTA (not shown). The NP-EGTA-induced block of chromosome segregation could be reversed in 22 of 27 embryos ($p = 0.015$, compared to controls [Fisher test]) by applying a flash of UV light (Figure 4D). NP-EGTA injection did not prevent, though it did delay, reformation of the nucleus. The timing of reformation of the nucleus in NP-EGTA-injected embryos was the same whether or not calcium was released by photolysis (Figure 4D, inset).

Chromosome segregation thus requires a $[Ca^{2+}]_i$ signal, as does cytokinesis. Reformation of the nucleus is calcium independent. The presence of a spindle and the observation that a single reformed nucleus can be found eccentrically placed at one spindle pole when the spindle had elongated strongly suggests that separation of the chromosomes is prevented by nondisjunction of sister chromatids, rather than by the absence of traction force within the spindle or loss of kinetochore-microtubule attachment.

An $InsP_3$ Receptor Antagonist Reversibly Blocks Chromosome Disjunction

Although it can certainly be argued that dibromoBAPTA and NP-EGTA are more likely to exert their effects through suppression of a calcium signal than by altering resting levels of $[Ca^{2+}]_i$, effects on resting $[Ca^{2+}]_i$ cannot be formally excluded. Another way of preventing calcium signals is to block the release of calcium from internal stores using heparin, an $InsP_3$ receptor antagonist (Ciapa et al., 1994). Microinjecting heparin into embryos just after NEB completely suppresses subsequent calcium signals, producing a block of chromosome separation (Figures 5A and 5B). A de-N-sulphated heparin control injection is without effect (Figure 5B). As with dibromoBAPTA and NP-EGTA, heparin-injected embryos often initiated a division furrow but failed to undergo cytokinesis and usually reformed a single nucleus as they left mitosis (Figures 5B and 5D). In embryos with a single mass of chromatin, the chromatin assumed an elongated ovoid form within the spindle (Figure 5D), as if the mitotic spindle were exerting a traction force on the chromatin. The nucleus often became eccentrically placed, consistent with force generation in the spindle with a block of chromosome disjunction. We compared heparin-injected embryos with embryos microinjected with VP16, a topoisomerase II inhibitor that prevents disjunction of sister chromatids (Holm et al., 1989; Shamu and Murray, 1992); the VP16-treated embryos showed a similar phenotype, with elongated ovoid nuclei

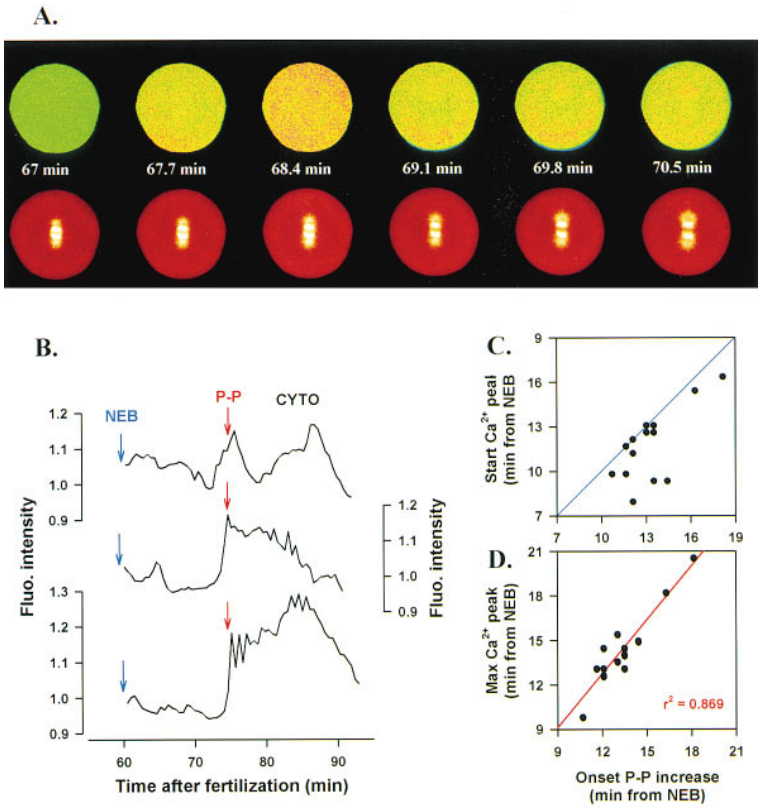

Figure 3. The $[Ca^{2+}]_i$ Increase Precedes Anaphase Onset

(A) Simultaneous confocal pseudoratio (see Experimental Procedures) CaGr fluorescence images of $[Ca^{2+}]_i$ (top row images) and microtubules (bottom row images) at the metaphase-anaphase transition, representative of 14 experiments. Embryos were injected in G2 with rhodamine-tubulin (50 μg/ml) followed by a second injection of calcium green-1 dextran (10 μM). Images were obtained every 28 s from late G2. Time in minutes from fertilization.

(B) Typical calcium traces at anaphase onset (red arrows, onset of P–P increase). NEB is normalized to 60 min (blue arrows).

(C and D) Comparison of the time when onset of spindle elongation takes place with the time when $[Ca^{2+}]_i$ begins to rise ([C], start Ca^{2+} peak) or reaches a maximum ([D], max Ca^{2+} peak). A linear regression is shown in (D) (regression line and coefficient, r^2, in red), while a line $y = x$ is drawn in (C) (blue line).

and eccentric placement, except that cytokinesis occurred, often producing an enucleate daughter cell (Figure 5D; Table 1). The block of cytokinesis by heparin suggests that $InsP_3$-driven calcium transients are necessary for maintenance of the cleavage furrow.

Heparin is a competitive inhibitor of $InsP_3$, so we reasoned that exogenous $InsP_3$ should reverse its effects. We coinjected a just-blocking dose of heparin (150 μg/ml) together with a photolysable $InsP_3$ derivative. A UV light flash applied to these embryos relieved the block to chromosome disjunction (Figure 5C). In five separate experiments, a total of 22 of 29 embryos completed chromosome separation when flashed with UV light ($p = 0.004$ compared to controls [Fisher test]), demonstrating that chromosome disjunction is triggered by $InsP_3$-induced calcium release at anaphase onset.

The UV light flash delivered at metaphase did not significantly rescue cytokinesis (28% of the flashed embryos formed two cells against 19% in the controls embryos, $p = 0.194$ [Fisher test]) implying that a separate, later calcium increase may be required for the completion of cytokinesis.

Table 1. Effect of DibromoBAPTA on Mitosis Onset

DiBrBAPTA (μM)[b]	Total (n)	2 nu[a], 2 cells	2 nu, 1 cell	1 nu, 1 cell	No nu, 1 cell
75	11	9 (82)[c]		2 (18)	
150	7	3 (43)	1 (14)	3 (43)	
300	20		2 (10)	17 (85)	1 (5)
600	16			7 (44)	9 (56)

[a] nu, nucleus; score with Hoechst DNA labeling after the reformation of the nuclear envelope.
[b] Final concentration in the embryos.
[c] n, number of embryos (% of Total [n]).

Heparin Delays, but Does Not Block, Spindle Elongation

We injected heparin into embryos whose microtubules and DNA were visualized in the confocal microscope using rhodamine tubulin and Hoechst dye to confirm that suppressing the anaphase calcium signal prevented chromosome disjunction, not spindle elongation. One of eight separate experiments is illustrated (Figure 6A). Chromosomes do not separate in heparin-injected embryos. The chromatin assumes an ovoid shape and is eventually dragged to one of the spindle poles. Spindle microtubules remain attached to the chromatin. Heparin delays spindle pole–pole elongation (Figure 6A) by around 10 min compared to controls (see Figure 2A) as it does astral microtubule elongation and reformation of the nuclear envelope (Figure 6A). The reorganization of the pericentriolar material that contributes to the AMT elongation (Figure 2A) is absent in the heparin-injected embryos, but centrosome duplication still occurs (Figure 6A).

We noted that spindle size (pole–pole distance at metaphase) was reduced in heparin-injected embryos (Figure 6B). It is known that smaller spindles lead to delayed mitosis and nuclear envelope reformation in sea urchin embryos (Sluder, 1979). Embryos were treated with sufficient colcemid to reduce the spindle size by an amount comparable to heparin, and the timing of mitosis in these colcemid-treated embryos was compared with controls (Figure 6B). As expected, colcemid-treated embryos showed a delay in anaphase onset

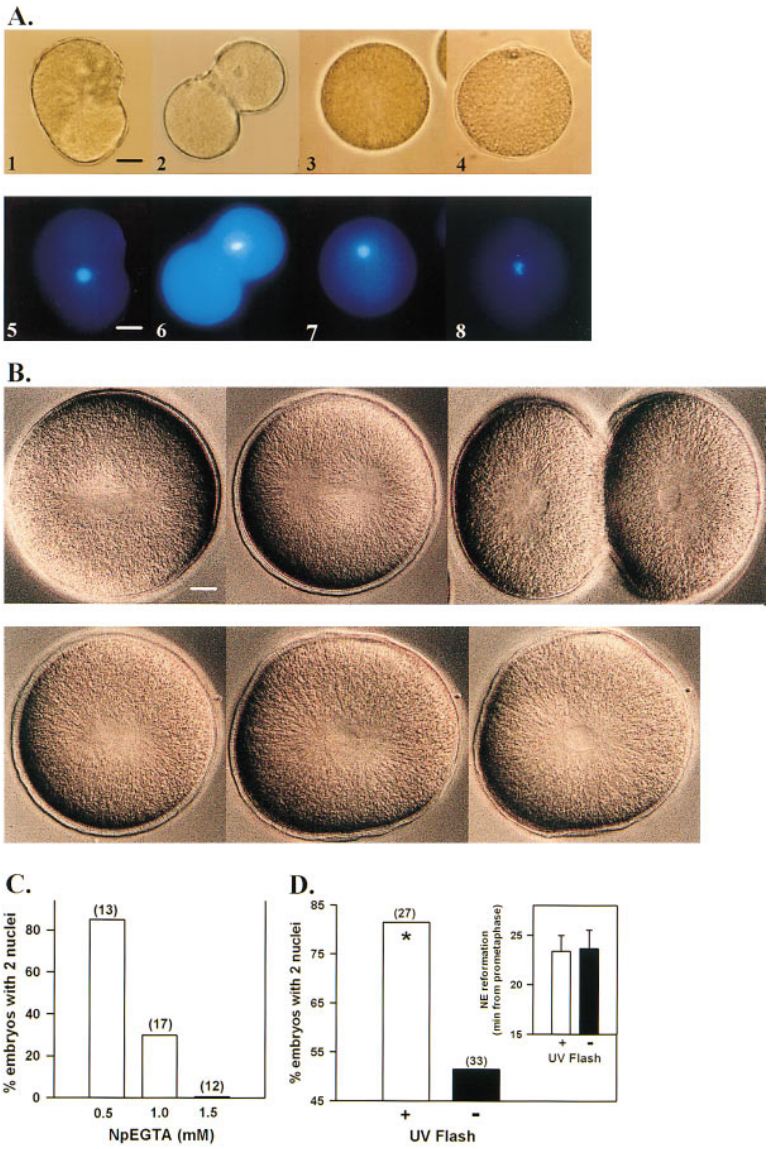

Figure 4. The Calcium Chelator, DiBrBAPTA, Reversibly Blocks Chromosome Disjunction

(A) Phenotype of embryos injected with 0.3 mM (pictures 1, 2, 5, and 6) or 0.6 mM (pictures 3, 4, 7, and 8) DiBrBAPTA (injection during prometaphase, pictures taken at least 100 min after fertilization). Pictures 1–4, bright field pictures. Pictures 5–8, same embryos in the fluorescence microscope after DNA staining with Hoechst. Scale bar = 20 μm.

(B) Differential interference contrast images of control embryos (top) and embryos microinjected with NP-EGTA (1 mM, bottom). The control embryo underwent anaphase onset at 100 min postfertilization. The mitotic spindle is visible in both control and NP-EGTA-injected embryos. NP-ETGA-injected embryos fail to cleave. A single centrally placed nucleus forms in this example by 120 min, when the control embryo has cleaved. In 5 of 16 embryos, the nucleus is finally located close to one of the spindle poles. Scale bar = 10 μm.

(C) Dose effect of prometaphase NP-EGTA injections on the formation of two nuclei.

(D) Reversibility of the calcium chelator's inhibitory effect in embryos injected with 1 mM NP-EGTA and the effect of calcium release on the timing of nuclear envelope (NE) reformation. Number in brackets, total number of embryos used to determine the percentage. *: Fisher statistical analysis ($p = 0.015$).

comparable to heparin-injected embryos (Figure 6B). These data indicate that the delay to mitosis and the nuclear cycle can be accounted for simply by an effect of heparin on mitotic spindle size.

Because heparin delays spindle elongation, the possibility that the effect on chromosome disjunction we observe may be due to UV cross-linking must be considered. This seems unlikely for two reasons. The first is that the behavior of the nucleus in these confocal experiments is identical to that seen in experiments in which heparin-injected embryos were not exposed to UV light until they were observed at the end of the experiment (Figure 5D). The second is that heparin-injected embryos received the same dose of UV light as controls between the start of the scan and the onset of P–P motion, as they were deliberately scanned less frequently.

Discussion

It has been proposed that a $[Ca^{2+}]_i$ increase may trigger anaphase onset (Izant, 1983; Poenie et al., 1986; Rattan et al., 1986; Whitaker and Patel, 1990; McIntosh and Hering, 1991), but the evidence has been open to question (Hepler, 1994; Morin et al., 1994). We show that an anaphase calcium signal provokes chromosome disjunction during first mitosis in sea urchin embryos. Spindle force generation and nuclear reformation are not calcium-triggered events. This observation may help explain earlier results.

Anaphase Calcium Signals in Sea Urchin Embryos

We used imaging methods to determine the properties and significance of the anaphase-related calcium signal that had previously been detected using whole cell recording techniques (Poenie et al., 1985; Ciapa et al., 1994). The anaphase signal is a global transient that can reach a concentration of around 1 μM in the cell periphery. The anaphase $[Ca^{2+}]_i$ increase is temporally homogeneous at our sampling frequency, but it does show spatial inhomogeneity in that the calcium concentration at the peak of the transient is only around 0.3

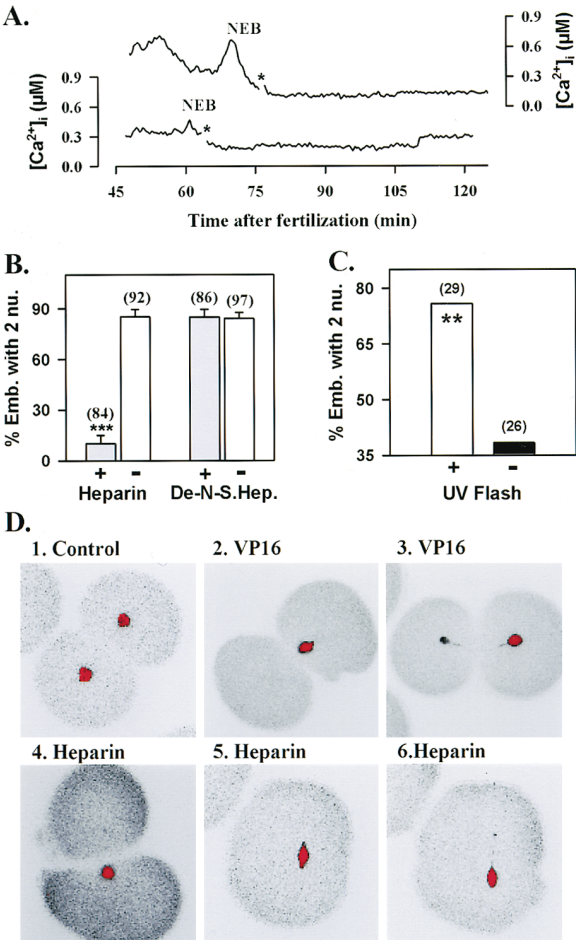

Figure 5. Calcium-Dependent Inhibition of Chromosome Separation by the $InsP_3$ Antagonist, Heparin

(A) Block of calcium release in heparin-injected embryos (representative of six experiments). $[Ca^{2+}]_i$ was measured using the confocal ratioing method (see Figure 1). *: prometaphase heparin injection (200 μg/ml final concentration).

(B) Chromosome separation is significantly blocked (***: $p < 0.001$ [Student's t test]) in embryos injected with heparin (200 μg/ml) when compared with either noninjected embryos (open bars) or with de-N-sulfated heparin (200 μg/ml)-injected embryos (determined by the reformation of two nuclei). Results from 12 separate experiments (number in brackets, total number of embryos).

(C) Release from the heparin-dependent block of chromosome separation through the photolysis of caged $InsP_3$ (10 μM injected in G2). A UV flash was (open bar) or was not (black bar) applied in metaphase to embryos previously injected in prometaphase with a minimal blocking concentration of heparin (150 μg/ml). Number in brackets, total number of embryos. **: $p = 0.004$ (Fisher test).

(D) Various phenotypes observed for embryos injected with VP16 (Topoisomerase II inhibitor, 100 μM) or with heparin. Pseudocolored confocal images of embryos stained with Hoechst (red, DNA). (5) and (6) represent the same embryo at 20 min intervals, where traction forces are first applied on the chromosomes (5) before the nucleus reforms at one pole (6).

μM in the region of the spindle compared to the 1 μM at the periphery, though the proportionate increase in $[Ca^{2+}]_i$ is the same throughout the cell. A standing gradient of calcium concentration seems to be maintained in the cell throughout mitosis, independent of the calcium signals superimposed upon it. We should be cautious about this finding, as the observation may in fact represent some unknown imaging artifact. However, we have used dextran-coupled indicator dyes and a ratiometric method. Moreover, control experiments with fluorescein dextran in place of calcium green dextran show no evidence of artifactual loss of ratio signal in the region of the spindle. Such a calcium gradient has also been observed in the PtK2 mammalian cell line using the fura2 ratio technique (Rattan et al., 1986). It may well be that a standing calcium gradient reflects the marked concentration of the endoplasmic reticulum, the calcium sequestering organelle, around the mitotic apparatus (Silver et al., 1980; Terasaki and Jaffe, 1991) and the activation of calcium sequestering mechanisms at mitosis (Suprynowicz and Mazia, 1985; Petzelt et al., 1987). This observation can resolve the paradox that calcium increases at mitosis but can also depolymerize spindle microtubules (Kiehart, 1981). It may be that the close association of the endoplasmic reticulum around the spindle fosters a microenvironment around microtubules in which $[Ca^{2+}]_i$ increases are modest, even as the cell as a whole experiences a larger calcium transient.

The Anaphase $[Ca^{2+}]_i$ Signal Correlates with and Causes Chromosome Separation

Anaphase onset and the anaphase-related calcium transient correlate well in experiments in which $[Ca^{2+}]_i$ and spindle microtubules are imaged simultaneously. Anaphase onset never occurs before $[Ca^{2+}]_i$ begins to rise and, in general, anaphase onset correlates well with the peak of the anaphase $[Ca^{2+}]_i$ transient. DibromoBAPTA, a calcium chelator, blocks chromosome separation, as does a photolysable calcium chelator, NP-EGTA. Photolysis of the NP-EGTA generates a calcium pulse (Wilding et al., 1996) and reverses the inhibition. Chromosome separation can also be prevented by microinjection of the $InsP_3$ receptor antagonist, heparin. The heparin block is reversed by generating a pulse of $InsP_3$ that competitively reverses the inhibitory action of heparin on the receptor. These observations indicate that the anaphase $[Ca^{2+}]_i$ signal causes chromosome separation.

Calcium can be seen to regulate chromosome disjunction, rather than force generation by the spindle, in agreement with current ideas about spindle function, where force is exerted even by the metaphase spindle (Rieder and Salmon, 1994; Khodjakov et al., 1996). This idea is graphically illustrated by the observation that the chromatin in heparin-injected embryos is eventually distorted into an ovoid shape by the pulling of the spindle microtubules and by the frequent observation of an eccentrically placed single nucleus in cells treated with calcium chelators. A similar behavior and appearance occurs in embryos treated with the topoisomerase II inhibitor, VP16. VP16 blocks disjunction at a stage distal in time to the dissolution of the "glue" that binds chromatid pairs at the kinetochore (Uemura et al., 1987; Bhat et al., 1996). We cannot say whether the calcium signal itself acts on the glue or at the later stage revealed by topoisomerase II inhibition.

Non-spindle-attached chromosomes in sea urchin embryos disjoin within minutes of their counterparts on

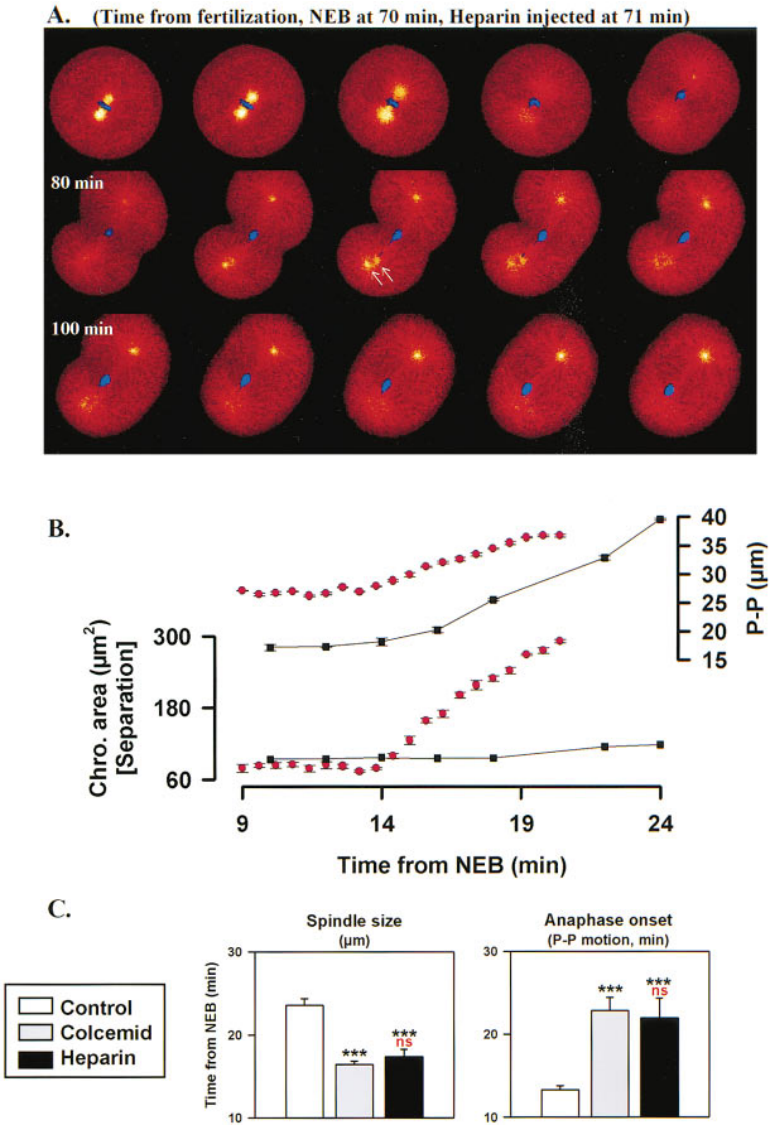

Figure 6. Delays of Spindle Elongation and Nuclear Cycle in Heparin-Injected Embryos

(A) Simultaneous confocal imaging (see Figure 2) of microtubules (pseudocolored in orange) and chromosomes (pseudocolored in blue) in a heparin-injected embryo (representative of eight experiments, sampling every 120 s, alternate display). White arrows, duplicated centrosomes.

(B) Spindle length and chromosome separation (shown as chromosome area) in the control embryo illustrated in Figure 2 (red) and in the heparin-injected embryo shown here (black).

(C) Spindles with comparably reduced size produced by colcemid ($n = 4$) or heparin ($n = 6$) treatment (left graph) show a similar anaphase onset delay compared to control embryos ($n = 9$). Student's t test (black, heparin/control comparison; red, heparin/colcemid) ***: $p < 0.001$; *: $p < 0.05$; ns, $p > 0.05$. Sampling every 28 s of tubulin images.

the mitotic spindle (Sluder et al., 1994). This observation is clearly consistent with a calcium signal causing chromosome disjunction. The slight 3–4 min delay to disjunction of nonattached chromosomes observed indicates that nonattached chromosomes are slightly slower to respond than spindle chromosomes, either because they are less sensitive to $[Ca^{2+}]_i$ or because calcium generates an activity at the metaphase plate that must diffuse toward the nonattached chromosomes.

The Anaphase $[Ca^{2+}]_i$ Transient Is Not Essential for Progression of the Nuclear Cycle

Blocking the anaphase $[Ca^{2+}]_i$ signal has dramatic consequences for chromatid separation but merely slows spindle elongation, chromatin recondensation, and reformation of the nuclear envelope. Indeed, the spindle continues to generate force, sometimes dragging the chromatin in its entirety toward one spindle pole. The delay to spindle elongation we observed appears to be due to the small size of the spindle in heparin-injected embryos; mimicking the spindle-size effect by colcemid treatment led to similar delays. The delay to nuclear reformation in heparin- and chelator-injected embryos may also be due to the effects of small spindle size on the nuclear cycle (Sluder, 1979, 1988). The important finding is that the nuclear cycle can run on in the complete absence of changes in $[Ca^{2+}]_i$. Indeed, calcium pulses generated by photolysis in NP-EGTA-injected embryos are sufficient to reverse the block of chromosome separation but do not significantly accelerate the timing of nuclear envelope reformation.

The delays in spindle elongation due to small spindle size were observed in dibromoBAPTA-, NP-EGTA-, and heparin-injected embryos but not in buffer-injected controls. Either these agents have some unknown direct effect on microtubule polymerization or, possibly, calcium is also involved in the process of spindle formation, as the close association of spindle microtubules with endoplasmic reticulum seems to imply (Terasaki and Jaffe, 1991). Indeed, calcium and the calcium-binding

protein, calmodulin, modify microtubule behavior (Keith et al., 1983; Sweet et al., 1988). It has also been reported that a protein, p62, regulated by a Ca^{2+}/calmodulin-dependent pathway is involved in microtubule dynamics in sea urchin embryos (Dinsmore and Sloboda, 1988).

Comparison with Data from Cell-Free Extracts

Events in the mitotic spindle have been studied in *Xenopus* cell-free extracts made with buffers containing the calcium chelator EGTA (Murray et al., 1996). Because the mitotic spindle can function normally in these calcium-chelating buffers, the view has developed that calcium signals are not required for mitotic progression (Morin et al., 1994). The data we present here are clearly inconsistent with this idea. It could thus be argued that the extracts do not faithfully reflect events in the living cell, but it is equally likely that local, endogenous calcium signals may, in fact, occur in extracts and promote anaphase onset. EGTA is not an effective antagonist of spatially discrete, transient calcium signals; BAPTA and, particularly, dibromoBAPTA are more effective (Speksnijder et al., 1989; Lindsay et al., 1995). Indeed, cell cycle progression in frog egg extracts is sensitive to these calcium chelators (Lindsay et al., 1995). Inactivation of mitotic H1 kinase activity is blocked by calcium chelators up to the point at which kinase activity is maximal; thereafter, inactivation is insensitive to chelators. It has also been shown in permeabilized sea urchin embryos that calcium addition in prophase of mitosis leads to H1 kinase inactivation, whereas later addition is without effect (Suprynowicz et al., 1994). Our experiments are consistent with these observations: microinjecting calcium chelators or heparin after NEB (when kinase activity is maximal) slows, but does not block, the reduction in H1 kinase activity, as evidenced by reformation of the nucleus. Equally, our finding that calcium release from NP-EGTA does not accelerate the nuclear cycle may merely reflect the fact that a late calcium pulse, though effective at triggering chromosome separation, arrives too late to affect the timing of the nuclear cycle.

Calcium Targets at Anaphase Onset

Our data demonstrate that chromosome separation can be prevented by interfering with the anaphase calcium signal, while spindle elongation, spindle force generation, and nuclear reformation are not absolutely dependent on the anaphase calcium increase. These observations imply that chromosome disjunction is controlled separately from events in the spindle itself and suggest that the signal that triggers the anaphase calcium transient also independently governs spindle elongation. Although the same pathways are involved in chromosome disjunction as in cyclin destruction at anaphase (Irniger et al., 1995), the events are dissociable in that chromosome segregation can occur in the absence of cyclin degradation (Holloway et al., 1993; Surana et al., 1993; Yamano et al., 1996). Chromosome disjunction in yeast and *Drosophila* requires destruction of Cut2 and PIM proteins, respectively (Funabiki et al., 1996; Stratmann and Lehner, 1996). Mutants of both genes show a nondisjunction phenotype, but cyclin is degraded normally. Nonetheless, just as for cyclin, the targeted proteolysis of the Cut2 protein involves the APC/proteasome ubiquitination proteolysis pathway (Funabiki et al., 1996). Inhibition of the anaphase calcium signal is thus formally equivalent to inhibition of the Cut2/PIM pathway, but we do not know whether the calcium signal is proximal or distal to Cut2/PIM destruction by the APC/proteasome. If it is proximal, then the calcium-independent activation of the cyclin/APC/proteasome pathway that leads to reformation of the nucleus in calcium-inhibited embryos must spare kinetochore-related proteolysis, perhaps through differential localization of elements of the proteolysis pathway in the cell. The simpler hypothesis is that the calcium signal is distal to, and caused by, Cut2/PIM destruction via activation of the APC/proteasome pathway. These alternatives can be tested.

There is evidence both in sea urchin embryos and mammalian cell lines that calmodulin/CaMKinaseII regulates mitosis (Baitinger et al., 1990; Lu and Means, 1993). It is likely that calmodulin is an immediate target of the anaphase calcium signal. In *Xenopus* eggs, a large fertilization calcium transient stimulates calmodulin/CaMKinaseII and, through them, the APC/proteasome (Lorca et al., 1993; Morin et al., 1994; reviewed in Whitaker, 1993). Calcium is known to activate the proteasome in ascidian eggs by conversion to the 26S form (Kawahara and Yokosawa, 1994). The analogy with *Xenopus* fertilization strongly suggests that the calcium signal is proximal to activation of the APC/proteasome pathway but can only be taken so far. The fertilization calcium in *Xenopus* is a large explosive wave triggered by the sperm, while at anaphase in the sea urchin embryo, the calcium signal is small, unwave-like, and endogenously generated. Moreover, the fertilization calcium signal is absolutely required for cyclin destruction and advance of the nuclear cycle (Lorca et al., 1993), whereas here, in mitotic anaphase, it is not essential for progression of the nuclear cycle. The absolute requirement for calcium in cyclin destruction at meiotic metaphase in *Xenopus* may reflect the fact that the unfertilized egg is blocked in meiotic metaphase by the *mos*-related cytostatic factor, which is absent in mitotic cell cycles (Sagata et al., 1989).

Mitotic Calcium Signals in Other Cell Types

Our observations in sea urchin embryos may explain some of the conflicting observations, described earlier, that have been reported on the role of calcium at anaphase onset. The effects of calcium chelators on spindle size can explain the slowing of anaphase onset and anaphase itself observed by others (Izant, 1983; Hepler, 1985). This colcemid-like effect is unrelated to calcium's role as a trigger of chromosome separation. Even with confocal imaging and nonsequestered dextran dyes, we find the anaphase calcium signal is small, at around 300 nM. Previous studies with permeating AM ester dyes (Tombes and Borisy, 1989; Kao et al., 1990) that are readily taken up into intracellular compartments may have lacked the sensitivity to detect a small signal. The lack of effect of permeant calcium chelators in previous studies may be explained by the relatively high levels of chelator required to block separation of the chromatids. We would not predict from our present results that

photorelease of calcium at metaphase would advance spindle elongation, and, indeed, no effect was found (Kao et al., 1990). Izant's early work (1983) reported that calcium injections could not induce chromosome disjunction in nocodazole-treated PtK1 cells. However, $[Ca^{2+}]_i$ was not monitored. Later work using more advanced methods is highly suggestive of the result reported here: Kao and coworkers (1990) reported an alteration in the appearance of the chromosomes when they released calcium by photolysis at metaphase. With hindsight, it may have corresponded to separation of the chromatids. We conclude that an anaphase calcium signal is present in mammalian somatic cells and predict that it will be found to induce separation of sister chromatids.

Experimental Procedures

Preparation of Gametes for Microinjection

Sea urchin eggs (*Lytechinus pictus*; Marinus, Long Beach, CA) were collected and developed at 16°C in artificial sea water (ASW: 435 mM NaCl, 40 mM $MgCl_2$, 15 mM $MgSO_4$, 11 mM $CaCl_2$, 10 mM KCl, 25 mM $NaHCO_3$, 1 mM EDTA, pH 8.0). Dejellied eggs were fertilized, stripped of their fertilization envelopes, and attached to glass coverslips with polylysine, as described previously (Becchetti and Whitaker, 1997).

Chemicals

5,5′-dibromo BAPTA (tetrapotassium salt, DiBrBAPTA) and fluorescent dyes were purchased from Molecular Probes (Eugene, OR). NP-EGTA was a gift from Dr. G. Ellis-Davies (Ellis-Davies and Kaplan, 1994). Heparin (H9399) and de-N-sulfated heparin (D4776) were from Sigma (Poole, Dorset, UK) and caged $InsP_3$ from Calbiochem (Nottingham, UK). The microinjection buffer was 0.5 M KCl, 20 mM Pipes, and 1 mM EGTA (pH 6.8). VP16 (Etoposide, Calbiochem), 10 mM in DMSO, was injected to give $<$1% DMSO in the cell; this concentration did not affect the cell cycle (data not shown).

Microinjection Procedure

Drawn borosilicate glass micropipettes (Clark Electromedical Instruments, GC150F-10) were manipulated with an Eppendorf micromanipulator (model 5171) and a piezoelectric advance (Märzhäuser Wetzlar, Germany). Solutions were pulsed into the embryos using gas pressure (pneumatic picopump, WPI, Hertfordshire, UK). Cytoplasmic concentrations were determined by evaluating cytoplasm displacement (0.1% to 1% pipette concentration; Wilding et al., 1996).

Flash Photolysis

A Cairn Research (Faversham, UK) flash photolysis system was used, attached to a Diaphot fluorescent microscope (Nikon, Telford, UK). Caged $InsP_3$ (10 μM in the embryo) was injected 20 min postfertilization (PF) and heparin (150 μg/ml in the embryo) injected in prometaphase (1 min after NEB). NP-EGTA was also injected in prometaphase. Three UV flashes (74 J) were applied to metaphase embryos (judged by the spindle appearance). Calcium release was detected using calcium green-1 dextran (1.5-fold increase). Nucleus reformation was scored using Hoechst DNA staining at the end of the experiment.

In Vivo Studies of Microtubules and Chromosomes

Rhodamine-labeled tubulin (dye/tubulin stochiometry: 1.0; low glycerol solution; Cytoskeleton, Denver, CO) was injected 20–25 min PF to 50 μg/ml. DNA was stained with Hoechst 33342 (2 μM, Sigma) added 40 min PF. Excitation was at 350 and 568 nm in a dual laser confocal microscope (Leica Lasertechnick GmbH, Heildelberg, Germany). Emitted light was analyzed with a dual dichroic mirror (DD488/568, Leica) and a 450 nm long pass filter, followed by a 450 band pass and a 585 long pass filter. 128 × 128 pixel images were collected every 36 s (8 line average scan). For rhodamine tubulin alone, 256 × 256 or 128 × 128 pixel images were collected every 28 or 23 s, respectively (16 line average). Measurements were made with morphometric software (Scanware 5.1, Leica). P–P distance was taken from one astral center to the other. AMT length is distance from astral centers to astral microtubule ends. Chromatid separation was determined by drawing an area (CA) around the chromosomes. Values are the average (μm or μm^2 ± SEM, n = 3).

Calcium Imaging and Ratio Measurements

Calcium green-1 dextran (CaGr, 10000 MW; Molecular Probes) was used to avoid internalization of the dye into intracellular compartments (Wilding et al., 1996). For the same reason, the dye was always injected 5 min before recording started, around 40 min PF. For CaGr/Rhodamine-tubulin experiments, both were injected 20–25 min PF. Excitation lines of 488 and 568 nm were used, with a DD488/568 dichroic mirror and a 510 nm long pass mirror with 530 nm band pass and 585 long pass filters. 128 × 128 pixel images were recorded every 28 s (16 line average). Cytoplasmic concentrations were: CaGr, 10 μM and Tetramethylrhodamine dextran (TMR, 10000 MW), 1 μM. 128 × 128 format images were recorded every 24 s (4 line average). $[Ca^{2+}]_i$ was calibrated as described previously (Wilding et al., 1996). Ratioed images were produced by dividing pixel by pixel the CaGr images by the TMR images, and pseudoratio images were obtained by dividing each subsequent image by the first image in the series (Gillot and Whitaker, 1994).

Colcemid Treatment

Partial depolymerization (spindle size reduced by 30%) was obtained after a 5 min incubation with 1 μM colcemid (Calbiochem; Sluder, 1979). The embryos were washed four times with ASW to remove the drug before microinjecting dyes.

Statistical Analysis

Statistical analyses used either Student's t test (1 tail, paired or unpaired as indicated) or Fisher's exact probability test, depending on the sample size.

Received August 1, 1997; revised December 8, 1997.

Acknowledgments

We are very grateful to Dr. G. Ellis-Davies for providing us with NP-EGTA. We thank Mr. M. Aitchison for his technical aid and his invaluable help with image processing, and Dr. G. Sluder for his thoughtful comments on the manuscript. Drs. I. Gillot and M. Wilding are kindly acknowledged for their helpful advice in the early work on the confocal microscope. This work was supported by grants from the Wellcome Trust.

References

Baitinger, C., Alderton, J., Poenie, M., Schulman, H., and Steinhardt, R.A. (1990). Multifuntional Ca^{2+}/calmodulin-dependent protein kinase is necessary for nuclear envelope breakdown. J. Cell Biol. *111*, 1763-1773.

Becchetti, A., and Whitaker, M. (1997). Lithium blocks cell cycle transitions in the first cell cycles of sea urchin embryos, an effect rescued by myo-inositol. Development *124*, 1099–1107.

Bhat, M.A., Philip A.V., Glover, D., and Bellen, H.J. (1996). Chromatid segregation at anaphase requires the *barren* product, a novel chromosome-associated protein that interacts with topoisomerase II. Cell *87*, 1103–1114.

Ciapa, B., Pesando, D., Wilding, M., and Whitaker, M. (1994). Cell-cycle calcium transients driven by cyclic changes in inositol trisphosphate levels. Nature *368*, 875–878.

Dinsmore, J.H., and Sloboda, R.D. (1988). Calcium and calmodulin-dependent phosphorylation of a 62 kd protein induces microtubule depolymerization in sea urchin mitotic apparatuses. Cell *53*, 769–780.

Elledge, S.J. (1996). Cell cycle checkpoints: preventing an identity crisis. Science *274*, 1664–1672.

Ellis-Davies, G.C.R., and Kaplan, J.H. (1994). Nitrophenyl-EGTA, a

photolabile calcium chelator that selectively binds calcium with high affinity and releases it rapidly on photolysis. Proc. Natl. Acad. Sci. USA *91*, 187–191.

Félix, M.-A., Labbé, J.C., Dorée, M., Hunt, T., and Karsenti, E. (1990). Triggering of cyclin degradation in interphase extracts of amphibian eggs by cdc2 kinase. Nature *346*, 379–382.

Funabiki, H., Yamano, H., Kumada, K., Nagao, K., Hunt, T., and Yanagida, M. (1996). Cut2 proteolysis required for sister-chromatid separation in fission yeast. Nature *381*, 438–441.

Gillot, I., and Whitaker, M. (1994). Calcium signal in and around the nucleus in sea urchin eggs. Cell Calcium *16*, 269–278.

Hartwell, L.H., and Weinert, T.A. (1989). Checkpoints: controls that ensure the order of cell cycle events. Science *246*, 629–634.

Hepler, P.K. (1985). Calcium restriction prolongs metaphase in dividing Tradescantia stamen hair cells. J. Cell Biol. *100*, 1363–1368.

Hepler, P.K. (1994). The role of calcium in cell division. Cell Calcium *16*, 322–330.

Hepler, P.K., and Callaham, D.A. (1987). Free calcium increases during anaphase in stamen hair cells of Tradescantia. J. Cell Biol. *105*, 2137–2143.

Herschko, A., Ganoth, D., Sudakin, V., Dahan, A., Cohen, L.H., Luca, F.C., Ruderman, J.V., and Eytan, E. (1994). Components of a system that ligates cyclin to ubiquitin and their regulation by the protein kinase cdc2. J. Biol. Chem. *269*, 4940–4946.

Holloway, S.L., Glotzer, M., King, R.W., and Murray, A.W. (1993). Anaphase is initiated by proteolysis rather than by the inactivation of maturing-promoting factor. Cell *73*, 1393–1402.

Holm, C., Stearns, T., and Botstein, D. (1989). DNA topoisomerase II must act at mitosis to prevent nondisjunction and chromosome breakage. Mol. Cell. Biol. *9*, 159–168.

Irniger, S., Piatti, S., Michaelis, C., and Nasmyth, K. (1995). Genes involved in sister chromatid separation are needed for B-type cyclin proteolysis in budding yeast. Cell *81*, 269–277.

Izant, J.G. (1983). The role of calcium ions during mitosis. Calcium participates in the anaphase trigger. Chromosoma *88*, 1–10.

Kao, J.P.Y., Alderton, J.M., Tsien, R.Y., and Steinhardt, R.A. (1990). Active involvement of Ca^{2+} in mitotic progression of Swiss 3T3 fibroblast. J. Cell Biol. *111*, 183–196.

Kawahara, H., and Yokosawa, H. (1994). Intracellular calcium mobilization regulates the activity of 26S proteasome during the metaphase-anaphase transition in the ascidian meiotic cell-cycle. Dev. Biol. *166*, 623–633.

Keith, C., DiPaola, M., Maxfield, F.R., and Shelanski, M.L. (1983). Microinjection of Ca^{2+}-calmodulin causes a localized depolymerization of microtubules. J. Cell Biol. *97*, 1918–1924.

Khodjakov, A., Cole, R.W., Bajer, A.S., and Rieder, C.L. (1996). The force for poleward chromosome motion in Haemanthus cells acts along the length of the chromosome during metaphase but only at the kinetochore during anaphase. J. Cell Biol. *132*, 1093–1104.

Kiehart, D.P. (1981). Studies on the in vivo sensitivity of spindle microtubules to calcium ions and evidence for a vesicular calcium-sequestering system. J. Cell Biol. *88*, 604–617.

King, R.W., Jackson, P.K., and Kirschner, M.W. (1994). Mitosis in transition. Cell *79*, 563–571.

King, R.W., Deshaies, R.J., Peters, J.-M., and Kirschner, M.W. (1996). How proteolysis drives the cell cycle. Science *274*, 1652–1659.

Li, X., and Nicklas, R.B. (1995). Mitotic forces control a cell-cycle checkpoint. Nature *373*, 630–632.

Lindsay, H.M., Whitaker, M.J., and Ford, C.C. (1995). Calcium requirements during mitotic cdc2 kinase activation and cyclin degradation in *Xenopus* eggs extracts. J. Cell Sci. *108*, 3557–3568.

Lorca, T., Galas, S., Fesquet, D., Devault, A., Cavadore, J.C., and Dorée, M. (1991). Degradation of the proto-oncogene product p39(mos) is not necessary for cyclin proteolysis and exit from meiotic metaphase: requirement for a Ca^{2+}-calmodulin dependent event. EMBO J. *10*, 2087–2093.

Lorca, T., Cruzalegul, F.H., Fesquet, D., Cavadore, J.-C., Méry, J., Means, A., and Dorée, M. (1993). Calmodulin-dependent protein kinase II mediates inactivation of MPF and CSF upon fertilization of *Xenopus* eggs. Nature *366*, 270–273.

Lu, K.P., and Means, A.R. (1993). Regulation of the cell cycle by calcium and calmodulin. Endocr. Rev. *14*, 40–58.

Luca, F.C., Shibuya, E.K., Dohrmann, C.E., and Ruderman, J.V. (1991). Both cyclin AΔ60 and BΔ97 are stable and arrest cells in M-phase, but only BΔ97 turns on cyclin destruction. EMBO J. *10*, 4311–4320.

McIntosh, J.R., and Hering, G.E. (1991). Spindle fiber action and chromosome movement. Annu. Rev. Cell Biol. *7*, 403–426.

Morin, N., Abrieu, A., Lorca, T., Martin, F., and Dorée, M. (1994). The proteolysis-dependent metaphase to anaphase transition: calcium/calmodulin-dependent protein kinase II mediates onset of anaphase in extracts prepared from unfertilized *Xenopus* eggs. EMBO J. *13*, 4343–4352.

Murray, A.W. (1992). Creative blocks: cell-cycle checkpoints and feedback controls. Nature *359*, 599–604.

Murray, A.W., Desai, A.B., and Salmon, E.D. (1996). Real time observation of anaphase in vitro. Proc. Natl. Acad. Sci. USA *93*, 12327–12332.

Nasmyth, K. (1996). Viewpoints: putting the cell cycle in order. Science *274*, 1643–1645.

Nicklas, R.B., Ward, S.C., and Gorbsky, G.J. (1995). Kinetochore chemistry is sensitive to tension and may link mitotic forces to a cell cycle checkpoint. J. Cell Biol. *130*, 929–939.

Nurse, P. (1994). Ordering S phase and M phase in the cell cycle. Cell *79*, 547–550.

Petzelt, C., Hafner, M., Mazia, D., and Sawain, K.W. (1987). Microtubules and Ca^{2+}-sequestering membranes in the mitotic apparatus. Eur. J. Cell Biol. *45*, 268–273.

Poenie, M., Alderton, J., Tsien, R.Y., and Steinhardt, R.A. (1985). Changes in the free calcium levels with stages of the cell division. Nature *315*, 147–149.

Poenie, M., Alderton, J., Steinhardt, R., and Tsien, R. (1986). Calcium rises abruptly and briefly throughout the cell at the onset of anaphase. Science *233*, 886–889.

Rattan, R.R., Shelanski, M.L., and Maxfield, F.R. (1986). Transition from metapahse to anaphase is accompagnied by local changes in cytoplasmic free calcium in PtK2 kidney epithelial cells. Proc. Natl. Acad. Sci. USA *83*, 5136–5140.

Rattan, R.R., Maxfield, F.R., and Shelanski, M.L. (1988). Long-lasting and rapid calcium changes during mitosis. J. Cell Biol. *107*, 993–999.

Rieder, C.L., and Salmon, E.D. (1994). Motile kinetochores and polar ejection forces dictate chromosome position on the vertebrate mitotic spindle. J. Cell Biol. *124*, 223–233.

Rieder, C.L., Schultz, A., Cole, R., and Sluder, G. (1994). Anaphase onset in vertebrate somatic cells is controlled by a checkpoint that monitors sister kinetochore attachement to the spindle. J. Cell Biol. *127*, 1301–1310.

Sagata, N., Watanabe, N., VandeWoude, G.F., and Ikawa, Y. (1989). The cmos proto-oncogene product is a cytostatic factor responsible for meiotic arrest in vertebrate eggs. Nature *342*, 512–518.

Shamu, C.E., and Murray, A.W. (1992). Sister chromatid separation in frog eggs extracts requires DNA topoisomerase II activity during anaphase. J. Cell Biol. *117*, 921–934.

Silver, R.B. (1989). Nuclear envelope breakdown and mitosis in sand dollar embryos is inhibited by microinjection of calcium buffers in a calcium-reversible fashion, and by antagonists of intracellular Ca^{2+} channels. Dev. Biol. *131*, 11-26.

Silver, R.B., Cole, R.D., and Cande, W.Z. (1980). Isolation of mitotic apparatus containing vesicles with calcium sequestering activity. Cell *9*, 505–516.

Sluder, G. (1979). Role of spindle microtubules in the control of cell cycle timing. J. Cell Biol. *80*, 674–691.

Sluder, G. (1988). Control mechanisms of mitosis: the role of spindle microtubules in the timing of mitotic events. Zool. Sci. *5*, 653–665.

Sluder, G., Miller, F.J., Thompson, E.A., and Wolf, D.E. (1994). Feedback control of the metapahse-anaphase transition in sea urchin zygotes: role of maloriented chromosomes. J. Cell Biol. *126*, 189–198.

Speksnijder, J.E., Miller, A.L., Weisenseel, M.H., Chen, T.-H., and

Jaffe, L.F. (1989). Calcium buffer injections block fucoid egg development by facilitating calcium diffusion. Proc. Natl. Acad. Sci. USA *86*, 6607–6611.

Steinhardt, R.A., and Alderton, J. (1988). Intracellular free calcium rise triggers nuclear envelope breakdown. Nature *332*, 364–366.

Stratmann, R., and Lehner, C.F. (1996). Separation of sister chromatids in mitosis requires the *Drosophilia* pimples product, a protein degraded after the metaphase/anaphase transition. Cell *84*, 25–35.

Suprynowicz, F., and Mazia, D. (1985). Fluctuation of the Ca^{2+}-sequestering activity of permeabilized sea urchin embryos. Proc. Natl. Acad. Sci. USA *82*, 2389–2393.

Suprynowicz, F.A., Prusmack, C., and Whalley, T. (1994). Ca^{2+} triggers premature inactivation of the cdc2 protein kinase in permeabilized sea urchin embryos. Proc. Natl. Acad. Sci. USA *91*, 6176–6180.

Surana, U., Amon, A., Dowzer, C., McGrew, J., Byers, B., and Nasmyth, K. (1993). Destruction of the CDC28/CLB mitotic kinase is not required for the metaphase-anaphase transition in the budding yeast. EMBO J. *12*, 1969–1978.

Sweet, S.C., Rogers, C.M., and Welsh, M.J. (1988). Calmodulin stabilization of kinetochore microtubule structure to the effects of nocodazole. J. Cell Biol. *107*, 2243–2251.

Terasaki, M., and Jaffe, L.A. (1991). Organization of the sea urchin egg endoplasmic reticulum and its reorganization at fertilization. J. Cell Biol. *114*, 929–940.

Tombes, R.M., and Borisy, G.G. (1989). Intracellular free calcium and mitosis in mammalian cells: anaphase onset is calcium modulated, but is not triggered by a brief transient. J. Cell Biol. *109*, 627–636.

Twigg, J., Patel, R., and Whitaker, M. (1988). Translational control of $InsP_3$-induced chromatin condensation during the early cell cycles of sea urchin embryos. Nature *332*, 366–369.

Uemura, T., Ohkura, H., Adachi, Y., Morino, K., Shiozaki, K., and Yanagida, M. (1987). DNA topoimsomerase II is required for the condensation and separation of mitotic chromosomes in *S. pombe*. Cell *50*, 917–925.

Whitaker, M. (1993). Sharper than a needle. Nature *366*, 211–212.

Whitaker, M., and Patel, R. (1990). Calcium and cell cycle control. Development *108*, 525–542.

Wilding, M., Wright, E.M., Patel, R., Ellis-Davis, G., and Whitaker, M. (1996). Local perinuclear calcium signals associated with mitosis-entry in the early sea urchin embryo. J. Cell Biol. *135*, 191–199.

Yamano, H., Gannon, J., and Hunt, T. (1996). The role of proteolysis in the cell cycle progression in *Schizosaccharomyces pombe*. EMBO J. *15*, 5268–5279.

Zhang, D.H., Wadworth, P., and Hepler, P.K. (1992). Modulation of anaphase spindle microtubule structure in stamen hair cells of Tradescantia by calcium and related agents. J. Cell Sci. *102*, 79–89.